

# Water Enrichment by H<sub>2</sub>O *ortho*-Isomer: Four-Photon and NMR Spectroscopy<sup>1</sup>

S. M. Pershin<sup>a,\*</sup>, A. F. Bunkin<sup>a</sup>, N. V. Anisimov<sup>b</sup>, and Yu. A. Pirogov<sup>b</sup>

<sup>a</sup> Wave Research Center Prokhorov General Physics Institute of RAS, Moscow, Russia

<sup>b</sup> Center for Magnetic Tomography and Spectroscopy MSU, Moscow, Russia

\*e-mail: pershin@orc.ru

Received September 30, 2008; in final form, October 6, 2008

**Abstract**—Ratio of H<sub>2</sub>O *ortho*-/*para*-spin-isomers in water of different treatment procedures (distilled or cavitation fountain) were studied by both Rayleigh wing four-photon spectroscopy and <sup>1</sup>H nuclear magnetic resonance (NMR) spectroscopy. Low-frequency gas-like rotational resonances were observed in the 0.1–1.5 cm<sup>-1</sup> (3–45 GHz) spectral range and NMR proton density was measured in both water samples. We established that the intensity of *ortho*-isomer line (6<sub>16</sub>–5<sub>23</sub>) 0.74 cm<sup>-1</sup> measured by four-photon spectroscopy increases by factor of ~3.5 after cavitation treatment of distilled water. Moreover, the proton density measured by NMR spectroscopy in the same sample grows on ~17%. We have suggested that the enrichment of the distilled water by *ortho*-H<sub>2</sub>O molecules was achieved due to cavitation bubbles collapse when the water passes through the supercritical state.

PACS numbers: 78.47.Fg, 78.47.Nj, 76.60.Pc

DOI: 10.1134/S1054660X09030104

It is known that *ortho*-/*para* nuclear spin isomers of H<sub>2</sub>O [1, 2], H<sub>2</sub>, and others molecules [3, 4] are differ due to orientation of the hydrogen spin. The *ortho*-isomer has parallel spin (the total nuclear spin is unity,  $J = 1$ ) and *para*-isomer—the total nuclear spin is zero,  $J = 0$ . According to the quantum statistics these isomers have the equilibrium *ortholpara* ratio (OPR) 3:1 in air at the room temperature [1–4]. Moreover, the *ortholpara* conversion is strongly forbidden in the dipole approximation. For instance, the liquid *para*-hydrogen can be storage for the several months without conversion into the *ortho*-isomer [3, 4, 6]. The presence of paramagnetic impurities reduces of the relaxation time to the equilibrium *ortholpara* ratio. Nevertheless, the divergence from the OPR equilibrium state for a long time was observed not only in the liquid hydrogen, but also in liquid water and in gas phase [7–9].

The *ortho*-H<sub>2</sub>O enrichment of water vapor up to OPR value 10:1 [7] and 5:1 [8] was achieved by the water vapor transportation over the porous surface. Interestingly that the measured relaxation time to the equilibrium state after condensation in the liquid water was a few hours [7]. In the [9] the *ortho*-H<sub>2</sub>O enrichment of water vapor was observed by variation of vapor humidity inside the tight box of the terahertz spectrometer. In the condense phase (the water weak solution (1:500) in the Ar matrix at cryogenic (6–30 K temperature) the non-equilibrium OPR was achieved by fast cooling of the matrix [10]. The relaxation time was reduced substantially by including of the paramagnetic

oxygen molecules in the gas before condensation. So, the 12 h relaxation time was measured in the matrix-solution with the relative concentration H<sub>2</sub>O:O<sub>2</sub>:Ar = 1:20:2000, when the oxygen molecules in the argon matrix exceeds the H<sub>2</sub>O one by factor of 20 [10].

Recently [11], the rotational resonances of H<sub>2</sub>O molecules inside a liquid water was observed by four-photon Raman spectroscopy of rotational transitions in the low frequency, 0–100 cm<sup>-1</sup> (0–3 THz) range. It was established that the rotational transitions frequencies coincide with the H<sub>2</sub>O resonance lines in a gas phase [12]. Further, the rotational lines of *ortho* and *para*-spin isomer of H<sub>2</sub>O was identified also. Later, the spin-selective interaction of H<sub>2</sub>O molecules with such biopolymers as the proteins and DNA was observed in its aqueous solution [13]. Crucially, that the existence of the coherent rotational motion of molecules in liquids was confirmed recently by using of pump-probe femtosecond technique [14].

In this paper, we present the experimental evidence of the *ortho*-H<sub>2</sub>O enrichment of liquid water, which passed through cavitation treatment procedure. To increase the reliability our study was carried out with the aid both four-photon nonlinear spectroscopy [11] and nuclear magnetic resonance (NMR) spectroscopy [1]. The <sup>1</sup>H NMR spectroscopy signal is proportional to the number of H<sub>2</sub>O molecules, which have the total spin value is 1, i.e., to the *ortho*-isomer concentration in water [1, 2].

In our experiments the two laser waves at frequencies  $\omega_1$  and  $\omega_2$ , whose difference  $(\omega_1 - \omega_2)/2\pi C$  ( $C$  is

<sup>1</sup> The article is published in the original.

the light velocity) is scanned in the low-frequency (negative and positive) spectral ranges. The parameter to be measured is the depolarization factor of radiation at the frequency  $\omega_s = \omega_1 - (\omega_1 - \omega_2)$ , whose nonlinear source is given by:

$$\mathbf{P}_i^{(3)} = 6\chi_{ijkl}^{(3)}(\omega_s; \omega_1; \omega_2; -\omega_1)\mathbf{E}_j^{(1)}\mathbf{E}_k^{(2)}\mathbf{E}_l^{(1)*}, \quad (1)$$

where,  $\chi^{(3)}$  is the cubic susceptibility of the medium, proportional to the correlation function of optical anisotropy fluctuations,  $\mathbf{E}^{(1)}$  and  $\mathbf{E}^{(2)}$  are the amplitudes of the interacting fields and  $I_s \propto |\chi^{(3)}|^2 I_1^2 I_2$  is the signal intensity. It must be emphasized that the probe laser field  $\mathbf{E}_l^{(1)*}$  interacts coherently with the ensemble of molecules that was prepared by the two laser fields  $\mathbf{E}^{(1)}$  and  $\mathbf{E}^{(2)}$ : second harmonic (532 nm) of Nd:YAG laser ( $\omega_1$ ) and dye laser ( $\omega_2$ ) respectively. This interaction controls the phases of the collective molecular motions in the volume, where the laser's beams with frequencies  $\omega_1$  and  $\omega_2$  overlap. The spectral resolution was  $\sim 0.1 \text{ cm}^{-1}$  and controlled by the dye laser's line width. The measurements were carried out in the range  $\pm 2 \text{ cm}^{-1}$ . Each experimental point was accumulated up to achievement of 5–10% accuracy of measurement. To achieve this accuracy value the 20–30 laser shots were used as a rule. The difference,  $(\omega_1 - \omega_2)/2\pi C$ , was tuned with spectral step of  $\sim 0.12 \text{ cm}^{-1}$ . The details of this technique are presented in the [11].

For convenient comparison we have studied both the distilled water and this water just after the cavitation procedure. We have used the commercial distilled water. Then the distilled water additionally purified by passing through an ion-exchange columns and porous filters (*Milli-Q*). Further, the cavitation treatment sample was prepared from *Milli-Q* water by spraying and subsequent condensation of aerosol generated in the ultrasonic cavitation fountain, which involves the cavitation process.

It is known [15] that water can be sprayed in a jet arising due to the fountain effect at the point where the beam of powerful ultrasonic waves, directed from the depth, hits the liquid surface. Periodic hydraulic impacts during cavitation bubble collapse excite capillary waves and provide detachment of aerosol microparticles at the fountain jet top. In this case, monodisperse aerosol is generated, which is easily observed visually as a fog. To generate aerosol in such a way, we used a focusing emitter made of a concave piezoceramic plate with a resonance frequency of 1.7 MHz. The emitter focal spot was slightly lower than the water surface and provided a pressure of about 10 MPa. Then this aerosol was condensed in a conventional way and collected into an air-tight plastic vessels stored in the tight box at room temperature before measurements.

The mass of both types of water samples is the same ( $506.0 \pm 0.5 \text{ g}$ ). The relative large volume and mass is

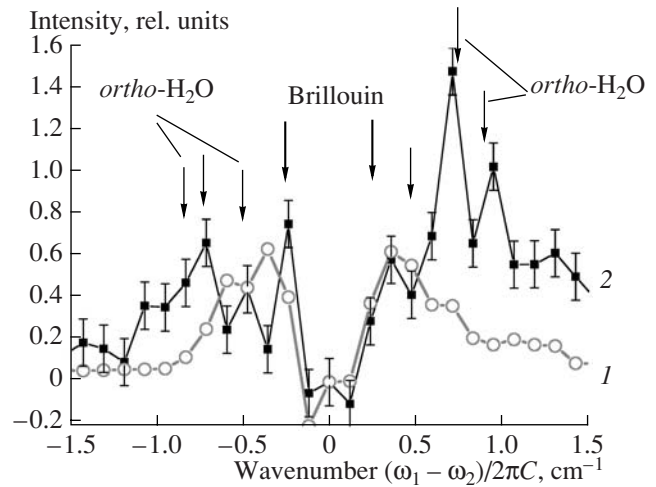


**Fig. 1.** The four-photon spectra of distilled water (open circles) and cavitation one (filled squares) after subtraction the contribution of Rayleigh components. Two lines in the middle of both spectra (marked by the thick arrows) are Brillouin resonances. Thin arrows mark the rotational lines ( $6_{16}-5_{23}$ ) ( $\pm 0.74 \text{ cm}^{-1}$ ), ( $5_{32}-4_{41}$ ) ( $\pm 0.87 \text{ cm}^{-1}$ ) and ( $4_{22}-3_{30}$ ) ( $\pm 0.4 \text{ cm}^{-1}$ ) of H<sub>2</sub>O molecule *ortho*-spin-isomer.

convenient to improve the signal to noise ratio in proton density measurement by NMR [1, 2]. Another portion of the water samples was used to the optical analysis by four-photon spectroscopy. All measurements were carried at the room temperature.

Four-photon scattering spectra in the range from  $-1.5$  to  $1.5 \text{ cm}^{-1}$  for distilled (open circles) and cavitation (filled squares) water samples are shown in Fig. 1. For convenience Fig. 1 illustrates the spectra after subtraction of Rayleigh scattering contribution to four-photon signal. Note that the Brillouin components in the both samples (mark by thick arrows) are almost similar on the amplitude value and its position. The strong and sharp lines at the frequency  $0.74$  and  $0.87 \text{ cm}^{-1}$  in the cavitation water (filled squares and standard deviation error bars) are attributed to the strongest H<sub>2</sub>O *ortho* spin-isomer lines (marks by thin arrows)  $0.74 \text{ cm}^{-1}$  ( $6_{16}-5_{23}$ ) and  $0.87 \text{ cm}^{-1}$  ( $5_{32}-4_{41}$ ) according to the HIT-RAN data base [12]. It should be emphasized that the intensity of the other *ortho*-isomer line  $0.4 \text{ cm}^{-1}$  ( $4_{22}-3_{30}$ ) is more than 1000 times smaller in comparison with the  $0.74 \text{ cm}^{-1}$  one [12]. Further, the *para*-isomer  $0.072 \text{ cm}^{-1}$  ( $4_{22}-5_{15}$ ) resonance has the  $\sim 10^{-5}$  part from the intensity of the  $0.74 \text{ cm}^{-1}$  line [12] and its contribution in the experimental spectra is negligible. The Brillouin resonances are located symmetrically in the both curves at the frequency  $\pm 0.25 \text{ cm}^{-1}$ , which is tabular value for the water [11, 13].

The comparison of the spectra in Fig. 1 shows that the cavitation water has the significantly higher intensity than the distilled one at *ortho*-spin-isomer reso-

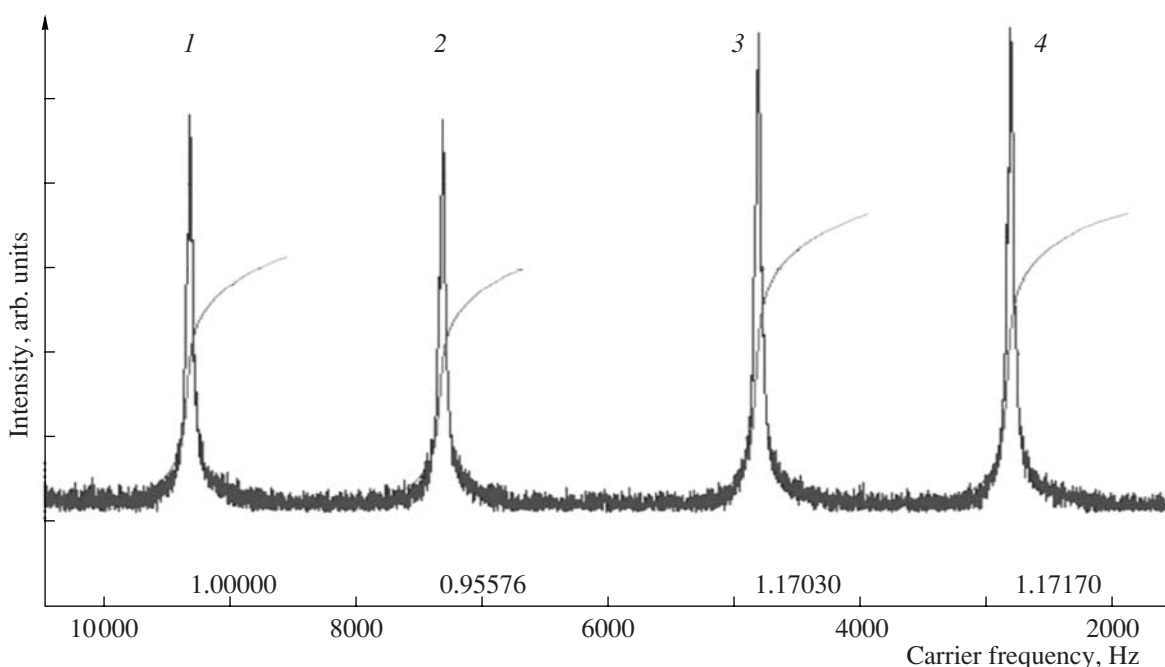


**Fig. 2.** NMR spectra of distilled water (1 and 2 curves) and cavitation water (3 and 4 curves) in proton density units. Thin S-like curve on all spectral lines shows the integral evolution through the lines and value of proton density. 1.00 and 0.96 (curve 1 and 2); 1.17 and 1.17 (curve 3 and 4), respectively. The ordinate axis is the signal intensity in arbitrary units.

nance with the frequency  $\pm 0.74 \text{ cm}^{-1}$ . The observed substantial difference can be interpreted undoubtedly as the enrichment of distilled water by *ortho*-isomer molecules by a factor of  $\sim 3.5$  after cavitation treatment when the water passes through the supercritical state due to the cavitation micro bubbles collapse. Really the chemical and physical processes following the cavitation micro bubbles collapse in condensed phases of water are rather poor understood, however it is known that the supercritical value of the temperature and pressure is reached during this process [16].

We checked this conclusion by nuclear magnetic resonance spectroscopy in the Center for Magnetic Tomography and Spectroscopy of Moscow State University, where we measured the proton density in the different water samples including cavitation and distilled water, as well as some commercially available types of water.

As mentioned above the  $^1\text{H}$  NMR spectroscopy allows us to direct measure of proton density value, which is proportional to  $\text{H}_2\text{O}$  *ortho*-isomer concentration in the water [1, 2], before and after its cavitation treatment. NMR spectroscopy of water samples was carried out with the aid of magnetic resonance image (MRI) scanner Tomikon-S50 (Bruker, 0.5-Tesla). Spectrum processing and integral calculation were carried out by off-the-shelf code XwinNMR v. 1.0. The samples have the same mass because the proton density depends on this parameter and were displaced in a plastic (0.5 l) bottles. To avoid the influence of magnetic

field gradient to the measurements the bottle was located in the same position inside the MRI-scanner.

Figure 2 shows the four characteristic NMR spectra of water in proton density units. Both samples were analyzed twice through 10 s interval between the events. The first two lines (Fig. 2, curves 1, 2) are attributed to NMR spectra of distilled water and the lines 3 and 4 to the cavitation one. Crucially, the NMR spectra of cavitation water (curve 3, 4) have the greater amplitudes in comparison with distilled one.

S-like thin curves in the Fig. 2 are proportional to the calculated integral value of these lines and equivalent to the proton density [1, 2]. The integral magnitude is normalized onto the first measurement of distilled water (curve 1, Fig. 2). These magnitudes are presented under the each line. One can see that the integral value in cavitation water is greater than in distilled one on  $\sim 17\%$ . We have interpreted this increasing of the proton density as the enrichment of the cavitation water by the *ortho*-isomer  $\text{H}_2\text{O}$  molecules.

Note that the similar measurement of proton density in the set of water samples, including tap and distilled water, commercial drinking water and distilled water with different concentration of paramagnetic gadolinium salt, which have the significant variability of their relaxation time, NMR integral values were the same within the accuracy  $\sim 2\%$ .

In summary the substantial (by factor of  $\sim 3.5$ ) increasing of amplitude of the  $\text{H}_2\text{O}$  *ortho*-isomers rota-

tional resonances both 0.74 cm<sup>-1</sup> (6<sub>16</sub>-5<sub>23</sub>) and 0.87 cm<sup>-1</sup> (5<sub>32</sub>-4<sub>41</sub>) have been observed for the first time to the best of our knowledge in water passes through the cavitation processes. Moreover this conclusion was confirmed by the detection of proton density arising up to ~17% after cavitation treatment of distilled water, which was measured by the nuclear magnetic resonance technique. Note that the proton density parameter is proportional to the H<sub>2</sub>O *ortho*-isomer concentration in the water samples.

The following interpretation seems plausible: The enrichment of distilled water by *ortho*-isomer H<sub>2</sub>O molecules occurs after cavitation treatment of water because it passes through the supercritical state—high temperature and pressure [16]. As follows from the theory [17], at a moment just before cavitation bubble collapse the pressure and temperature inside the bubble increase dramatically and reach the value ~10<sup>10</sup> Pa and ~10<sup>4</sup> K respectively. At this particular moment the most part of water molecules inside the bubble convert to such species as OH, O, O<sub>2</sub>, O<sub>3</sub>, H, H<sub>2</sub>, HO<sub>2</sub>, H<sub>2</sub>O<sub>2</sub>. Crucially, the half of H<sub>2</sub>O molecules dissociate into OH and H radicals [17]. After the recombination of these radicals and relaxation to the equilibrium state the *ortho/para* ratio must be 3:1 according to the quantum statistics, i.e. larger than in liquid water at the ambient conditions. This mechanism could be the reason of distilled water *ortho*-spin-isomer enrichment by cavitation procedure.

#### ACKNOWLEDGMENTS

This work was supported by RFBR Projects 07-02-12209, 08-02-00008, RAS Program “Optical Spectroscopy and Frequency Standards” as well as by a grant from the President of the Russian Federation supporting of leading scientific schools (no. NSh-8108.2006.2).

#### REFERENCES

1. N. Bloembergen, E. Parcell, and V. Pound, Phys. Rev. **78**, 679 (1948).
2. A. Losche, *Nuclear Induction* (Deutsch. Verlag Wissenschaften, Berlin, 1961).
3. A. Farkas, *Orthohydrogen, Parahydrogen, and Heavy Hydrogen* (Cambridge Univ., Cambridge, 1935).
4. H. H. Limbach, G. Buntkowsky, J. Matthes, et al., Chem. Phys. Chem. **7**, 551 (2006).
5. A. Miani and J. Tennyson, J. Chem. Phys. **120**, 2732 (2004).
6. P. L. Chapovsky and L. J. Hermans, Ann. Phys. Chem. **50**, 315 (1999).
7. V. I. Tikhonov and A. A. Volkov, Science **296**, 2363 (2002).
8. E. V. Stepanov, V. I. Tikhonov, and V. A. Milayev, Quant. Electron. **35** (3), 205 (2005).
9. X. Xin, H. Altan, A. Saint, D. Matten, and R. R. Alfano, J. Appl. Phys. **100**, 094905 (2006).
10. X. Michaut, A.-M. Vasserot, and L. Abouaf-Marguin, Vibrat. Spectrosc. **34**, 83 (2004).
11. A. F. Bunkin and S. M. Pershin, J. Raman Spectr. **39**, 726 (2008).
12. L. S. Rothman, D. Jacquemart, A. Barbe, D. Ch. Benner, M. Brick, L. R. Brown, M. R. Carleer, C. Chackerian, Jr. K. Chance, L. H. Coudert, V. Dana, V. M. Devi, J.-M. Flaud, R. R. Gamache, A. Goldman, J.-M. Hartmann, K. W. Jucks, A. G. Maki, J.-Y. Mandin, S. T. Massie, J. Orphal, A. Perrin, C. P. Rinsland, M. A. H. Smith, J. Tennyson, R. N. Tolchenov, R. A. Toth, J. V. Auwera, P. Varanasi, and G. Wagner, J. Quant. Spectr. Radiant. Transfer **96**, 139 (2005); [www.elsevier.com/locate/jqsrt](http://www.elsevier.com/locate/jqsrt).
13. A. F. Bunkin, A. A. Nurmatov, and S. M. Pershin, Laser Phys. Lett. **3** (6), 275 (2006).
14. A. C. Moskun, A. E. Jailaubekov, S. E. Bradforth, G. Tao, and R. M. Strat, Science **311**, 1907 (2006).
15. A. F. Bunkin, S. M. Pershin, and L. N. Rashkovich, Opt. Spectrosc. **96**, 568 (2004).
16. M. P. Brenner, S. Hilgenfeldt, and D. Lohse, Rev. Mod. Phys. **74**, 425 (2002).
17. K. Yasui, Phys. Rev. E **56**, 6750 (1997).